

Freeform Extrusion Fabrication of Titanium Fiber Reinforced Bioactive Glass Scaffolds

Albin Thomas¹, Krishna C.R. Kolan¹, Ming C. Leu¹ and Gregory E. Hilmas²

¹Department of Mechanical and Aerospace Engineering, Missouri University of Science and Technology, Rolla, MO 65409

²Department of Material Science and Engineering, Missouri University of Science and Technology, Rolla, MO 65409
REVIEWED

Abstract

Although implants made with bioactive glass have shown promising results for bone repair, their application in repairing load-bearing long bones is limited due to their low fracture toughness and fairly fast degradation response *in vivo*. In this paper, we describe our investigation of freeform extrusion fabrication of silicate based 13-93 bioactive glass scaffolds reinforced with titanium fibers. A composite paste was prepared with 13-93 bioactive glass filled with titanium fibers (~16 μm in diameter and aspect ratio of ~250) having a volume fraction of 0.4 vol. %. This paste was then extruded to fabricate scaffolds with an extrudate diameter of about ~0.8 mm. The sintered scaffolds, with and without titanium fibers, had measured pore sizes ranging from 400 to 800 μm and a porosity of ~50%. Scaffolds produced with 0.4 vol. % titanium fibers were measured to have a fracture toughness of ~0.8 $\text{MPa}\cdot\text{m}^{1/2}$ and a flexural strength of ~15 MPa. Bioactive glass scaffolds without titanium fibers had a toughness of ~0.5 $\text{MPa}\cdot\text{m}^{1/2}$ and strength of ~10 MPa. The addition of titanium fibers increased the fracture toughness of the scaffolds by ~70% and flexural strength by ~40%. The scaffolds' biocompatibility and their degradation in mechanical properties, *in vitro* were assessed by immersing the scaffolds in a simulated body fluid over a period of one to four weeks.

1. Introduction

Bioactive glasses have been widely investigated for bone repair applications, because of their inherent capability to enhance new bone formation and the ability to bond to surrounding tissues [1]. Out of a variety of bioactive glasses, 13-93 bioglass is a silicate based glass (53 SiO₂, 20 CaO, 4 P₂O₅, 6 Na₂O, 12 K₂O, and 5 MgO, with chemical composition in weight. %) which has been thoroughly researched in the past and FDA approved for its proven chemical durability, bioactivity, bone cell proliferation and differentiation and more importantly its ability to be fabricated into scaffolds. Fu *et al.*[2], Liu *et al.*[3], Kolan *et al.*[4], Doiphode *et al.*[5], and Rahaman *et al.*[6] studied the use of 13-93 bioglass in fabricating scaffolds for bone repair using a variety of fabrication techniques including slip casting, polymer foam replication, selective laser sintering, freeze extrusion fabrication, and robocasting, respectively. The investigation into mechanical and biological properties of the fabricated scaffolds has shown that 13-93 bioglass has favorable properties in repairing load bearing bone defects [7, 8]. *In vivo* assessment of 13-93 bioglass has shown good bonding between the scaffold and the surrounding tissues, in addition to new bone and tissue growth around the scaffold [9-11]. A 30% reduction in compression strength was reported upon immersion of the 13-93 bioglass scaffolds in simulated body fluid for four weeks primarily because of the conversion of the 13-93 bioglass into hydroxyapatite (HA) [12]. Though the degradation has reportedly slowed down after two weeks and in fact, a recent long term *in vivo* assessment by Yinan et al. [13] showed that about half of

the scaffold still remains unconverted after 6 months of implantation in rat calvarial defects. Thus making the 13-93 bioglass a potential material to fabricate an implant for long term load bearing repair.

Previous studies on hot pressing of bioglass-metal composites have shown that the flexural strength and toughness of composite improved upon dispersion of metallic particles in the glass matrix [13-16]. Unsuccessful attempts to produce such composites by pressure less sintering were previously reported in the literature which could have been failed due to differences in the thermal properties of the glass and the metal. Also, there have been no reports of manufacturing such composite parts for biomedical applications using extrusion based additive manufacturing processes. As to provide more structural integrity for the scaffolds, we investigate addition of ductile titanium (Ti) metallic fibers into the 13-93 bioglass matrix to form a composite with improved toughness. Ti is used due to the following reasons: 1) Ti is an FDA approved, and widely used material for synthetic implants as it offers excellent biocompatibility; 2) there is only a small difference in the thermal expansion coefficients of 13-93 bioglass and Ti fibers; and 3) the presence of silica in 13-93 bioglass matrix and titanium oxide on the surface of titanium fibers will essentially provide good adhesion between these materials, thereby reducing problems like de-bonding. Therefore, the addition of metallic fibers is expected to improve the toughness of the implant and avoid a catastrophic failure during the bone repair process.

Several additive manufacturing techniques have been used in the past to fabricate scaffolds. Robocasting was used by Cesarano *et al.* to fabricate lattice scaffolds for load-bearing bone repair [19]. Simpson *et al.* [20] and Kolan *et al.* [21, 22] studied the effect of pore sizes and pore geometry on mechanical and biological properties of scaffolds manufactured by selective laser sintering. Foam replication technique was used by Chen *et al.* [23] to fabricate highly porous (90%) scaffolds. However the scaffolds fabricated using the above additive manufacturing techniques had low toughness compared to conventional methods like hot pressing. 3D printing of composites, especially, bioglass and metal composites, is relatively unexplored and acquiring further importance with the advent of several successful extrusion based techniques.

This study aims at fabricating Ti reinforced glass scaffolds using freeform extrusion. An aqueous paste mix of 13-93 bioglass, additives and Ti fibers were made for extrusion. Two sets of scaffolds, one with fiber (0.4 vol. %) and other one without fiber were fabricated and their heat treatment schedule was identified. Following this a comprehensive evaluation of its mechanical and biological properties was performed.

2. Materials and methods

2.1 Fabrication of scaffolds

The as-received water quenched 13-93 bioglass (Mo-Sci Corp, Rolla, MO) was crushed in a steel shatterbox (SPEX SamplePrep Crusher, Model 8500, Metuchen, NJ) and attrition-milled using de-ionized water for 3 h with ZrO₂ as the grinding medium. The particle size distribution was measured using a laser diffraction-based particle size analyzer (Model LS 13 320, Beckman Coulter Inc., Fullerton, CA). To make an extrudable paste, additives were added to the glass and then wet ball milled together overnight. Following milling, the mixture was heated for about 50 min at 70°C with continuous stirring along with the simultaneous addition of

binder (Methocel). For preparing a paste with fibers, the as-received long fibers were crushed using a porcelain mortar and pestle crusher with moderate force and then added to the stirring mix along with Methocel. This ensured uniform dispersion of fibers within the paste. Following this the paste was vacuum mixed for 4-5 min (WhipMix Vacuum Power Mixer Plus, WhipMix Corporation, Louisville, KY) to remove any air bubbles and then transferred into an air-tight container. The paste composition is provided in Table 1.

Table 1. Titanium reinforced 13-93 bioglass paste composition

Component	Concentration (vol. %)	Manufacturer
13-93 Glass particles	40	Mo-Sci Corp, Rolla, MO
Darvan C	2	Vanderbilt Minerals LLC, Norwalk, CT
Methocel	4.0 - 4.4	Dow Chemical Company, Midland, MI
Titanium fiber	0.0 - 0.4	Intramicron LLC, Auburn, AL
De-ionized water	54	-

A three-syringe independent extruder developed at Missouri S&T is used for fabrication of scaffolds. It primarily consists of extrusion devices, a motion subsystem and a real-time control system. The printer has X, Y, and Z-axes motion capabilities controlled by three stepper motors (Empire Magnetics, Rohnert Park, CA). A ram extruder is used to provide the extrusion force. The paste in a syringe (60 cc plastic syringe) is extruded through a 1.19 mm nozzle (Nordson EFD, Westlake, OH) on to a hot plate set at 40°C. After the completion of a layer, the gantry moves up by the thickness of one layer. These steps are repeated until the entire part is formed. A 40 x 36 x 6 mm³ scaffold with ~800 μm pore size and 0.7 mm layer height was fabricated.

2.2 Post processing and characterization of scaffolds

Thermogravimetric analysis (TGA) (NETZSCH thermal analyzer STA 409, Burlington, MA) was performed on the ‘green parts’ made, with and without Ti fiber, in order to identify the post processing schedule. The heating rate, temperature holds, and sintering temperature were determined from the TGA results. The pore sizes of the sintered scaffolds were measured using optical microscopy. The apparent porosity of the sintered scaffolds was measured using Archimedes method. X-ray diffraction (Philips X-Pert, Westborough, MA), run over 2θ range of 10° – 90° was used to identify the amorphous nature of sintered glass as well as the presence of Ti, using Cu Kα radiation ($\lambda = 0.154056$ nm). Surface of Ti fibers was examined for presence of oxides using X-ray photoelectron spectrometer (Kratos Axis 165 Photoelectron Spectrometer, Manchester, UK).

2.3 Mechanical testing of scaffolds

Scaffolds (3 x 5 x 25 mm³) with different volume fractions of titanium fibers were tested in flexure using an Instron testing machine (model 5881, Norwood, MA). Prior to testing, surface grinding (FSG-618, Chevalier Machinery Inc., Santa Fe Springs, CA) was done to prepare parallel surfaces. A four point semi-articulated fixture (outer span of 20 mm and inner span of

10 mm) at a cross-head speed of 0.2 mm/min using a 2 kN load cell was used in the flexure test and the load was applied along the z direction. The flexural stress was determined using the following equation (ASTM C1674-11):

$$\sigma = \frac{3Pl}{4bd^2}$$

where P is the applied force, l is the length of the outer span, b is the width and d is the thickness of the sample. The strength of the samples tested is expressed as mean \pm standard deviation (SD).

A Chevron notched beam test was used to assess the fracture toughness of the scaffolds ($3 \times 5 \times 25 \text{ mm}^3$). A notch was made at the mid-span of the scaffold using a dicing saw (Accu-Cut 5200, AREMCO Products Inc., Ossining, NY) with a 0.15 mm thick diamond blade. A four-point, semi-articulated fixture mentioned above was used for this testing too. The fracture toughness was calculated using the following equation (ASTM C1421-10):

$$K_c = F_m Y^*_{\min}(S_o - S_i) 10^{-6} / BW^{3/2}$$

where K_c is the fracture toughness, F_m is the maximum load, S_o and S_i are outer and inner spans of the fixture used, B is the depth, and W the width of the specimen. Y^*_{\min} is the minimum of the geometric function (calculated based on ASTM C1421-10 guidelines). At least five samples were tested and the toughness is expressed as mean \pm SD.

2.4 SBF tests on scaffolds

For *in vitro* assessment two sets of scaffolds were used, one set without fiber and the other set with fiber. The scaffolds ($5 \times 5 \times 5 \text{ mm}^3$) were cleaned thrice in distilled water, then in ethanol using an ultrasonic cleaner (Crest CP 500T, Trenton, NJ), and then dried overnight at 65°C . The scaffolds were then weighed and immersed in simulated body fluid (SBF) prepared according to the Kokubo method with a starting pH of 7.40. 100 ml of SBF solution was used per gram of the scaffold, and the scaffolds along with SBF solution were stored in plastic Nalgene bottles [24]. The samples were then kept in an incubator maintained at 37°C . Scaffolds were removed every week until four weeks and then dried overnight before weight and strength were assessed. Five samples per set were used in the compression testing and the strength is expressed as mean \pm SD. Scanning electron microscopic (Hitachi S-4700 FESEM, Hitachi Co., Tokyo, Japan) images were taken to study the surface morphology of the scaffolds. The scaffolds removed from SBF were tested in compression using an Instron testing machine (model 5881, Norwood, MA) at a crosshead speed of 0.5 mm/min using a 10 kN load cell. At least five samples were used in the compressive strength measurements and results were reported as mean \pm SD.

3. Results and Discussion

3.1 Fabrication of scaffolds

The size distribution of attrition milled glass particles is shown in Figure 1.a. The particle size varied from ~ 0.2 to $\sim 12 \mu\text{m}$ with an average of $2.3 \mu\text{m}$. The SEM image of the milled bioglass and the as-received titanium fibers are shown in Figure 1.b and 1.c, respectively. A typical irregular shape of the milled glass particles can be observed which will aid in achieving appropriate viscous flow characteristics during sintering. This could potentially reduce the micro

pores in the scaffolds [25]. The Ti fibers used in this study had an average diameter of 16 μm and aspect ratio of 250.

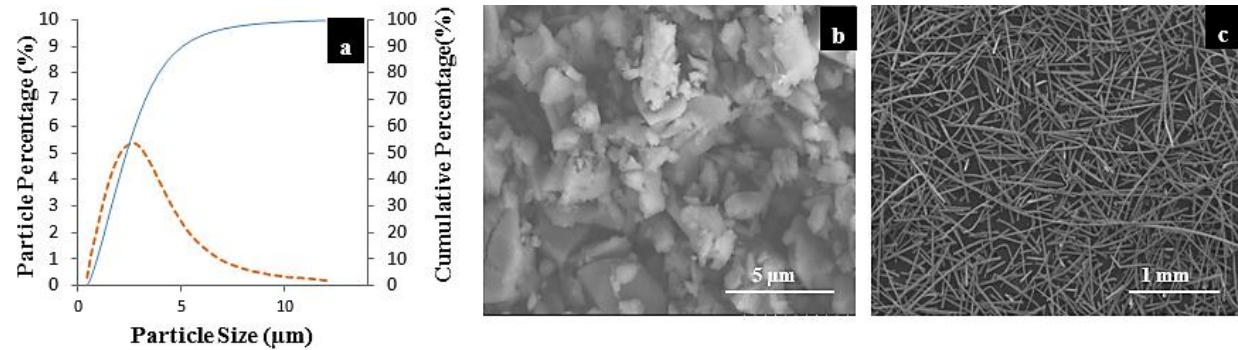


Figure 1. (a) Particle size distribution of attrition milled bioglass (b) SEM image of the attrition milled 13-93 bioglass (c) SEM image of as-received titanium fibers.

The fabrication process consists of three basic steps: preparing the paste, printing the scaffolds and sintering them. 13-93 bioglass+Ti composite paste was prepared with varying volume content of the Ti fibers from 0.1% to 0.5% in increments of 0.1%. The volume content was kept at 0.4% as a further increase in the Ti fiber content consistently blocked the needle and caused difficulties during the fabrication. The prepared paste (Figure 2.a) is filled into a syringe (manually) and is extruded onto a hot plate maintained at 40°C using layer-by-layer deposition through a 1.19 mm diameter nozzle (Nordson EFD, Ohio, USA). Scaffolds were fabricated using the extrusion fabrication machine shown in Figure 2.b. The extrusion force varied between 200-320 N based on the amount of titanium fibers in the paste and the viscosity of the paste. An as-fabricated scaffold with a 0.4% volume fraction of fibers is depicted in Figure 2.c. The green scaffold was 40 mm x 36 mm x 6.0 mm in size and the pore sizes varied from 750 to 1000 μm .

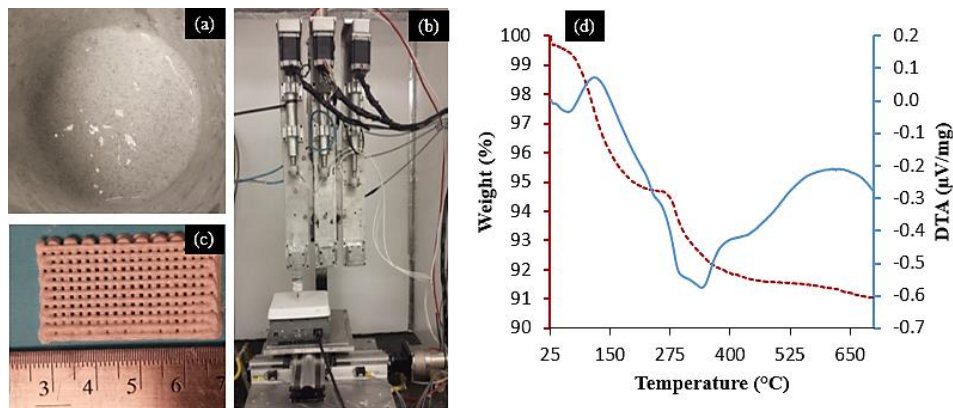


Figure 2. Steps in fabrication of scaffolds: (a) paste prepared with titanium fibers dispersed in bioglass; (b) Machine and syringe filled with paste used in fabrication of scaffolds; (c) As-fabricated scaffold; (d) Thermogravimetric analysis of paste used.

The binder burnout schedule for the ‘green scaffold’ was developed from the TGA curve in Figure 2.d. This curve shows the changes in weight of the ‘green scaffold’ as a function of increasing temperature. Noticeable changes in the weight of the scaffold were observed at

approximately 100 °C and 300 °C. The residual water evaporates at 80-120 °C and Methocel and Darvan C burn out at around 300-350 °C. Holding temperatures were designed based on the curve, as to aid slow burn-out of the additives in the scaffold. These observations were used to prepare the binder burnout and sintering schedule in Table 2.

Table 2. Binder burnout/sintering schedule used for scaffolds fabricated

Starting Temperature (°C)	Ending Temperature (°C)	Rate (°C/min)	Hold Period (h)
20	350	0.3	2
350	700	2	1
700	50	10	-

A slower heating rate is adopted in the binder burnout process so as to allow sufficient time for the decomposition of the organic additives. Figure 3.a shows a scaffold that underwent the binder burnout process at a faster heating rate of 5 °C/min (for 20 °C to 350 °C segment). The part turned black. This is mostly due to the trapped carbon from the organic additives. A sintered scaffold with 0.4 vol. % fiber that underwent the binder burnout schedule in Table 2 is pictured in Figure 3.b. A slow heating rate provides sufficient time for the additives to decompose from the fabricated part. The average shrinkage observed in the sintered scaffolds was measured to be ~25%, ~29% and ~17%, along the length, width, and thickness, respectively. The pore sizes varied from 600-850 µm. Optical images of the sintered scaffolds (Figure 3.c, d) reveal that the fibers are dispersed in the glass matrix. Figure 3.d shows the sintered part a higher magnification. The Ti fibers oriented along the direction of the extruded filament can also be clearly observed. The porosity of the scaffolds was measured to be ~58% based on the Archimedes method. Also, the XRD patterns of the sintered glass scaffold and the as-received glass particles indicated no crystallization and the glass retained its amorphous nature.

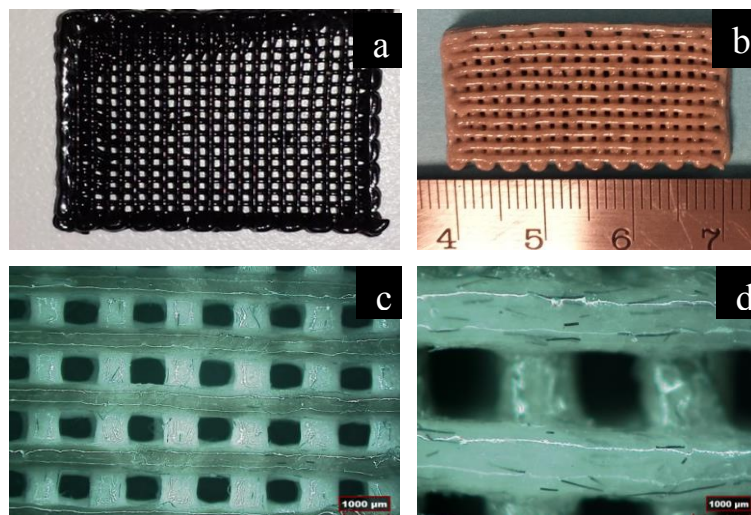


Figure 3. (a) Scaffold that turned black after undergoing binder burnout at a faster rate (5 °C/min); (b) Sintered 13-93 bioglass scaffold with 0.4 vol. % titanium fibers; (c) & (d) Optical image of the scaffold in (b) with its zoomed version

3.2 Assessment of mechanical properties of scaffolds

The flexural strength, flexural modulus and fracture toughness of scaffolds with varying vol. % of fibers is pictured in Figure 4. The flexural strength varied from ~10 MPa (0 vol. % of Ti fibers) to ~15 MPa (0.4 vol. % of Ti fibers). The flexural strength increased as the Ti fiber volume fraction increased. Previous mechanical testing studies on 13-93 bioglass scaffolds prepared by robocasting have shown that the value of flexural strength of 13-93 bioglass scaffolds is in the range of 11 ± 3 MPa which are consistent with the values obtained in this study [8]. The flexural modulus of the scaffolds increased to 15 GPa from 11 GPa due to addition of 0.4 vol. % Ti fibers into the scaffold. The trend in flexural modulus clearly shows that the flexural strength is increasing with addition of fibers. The flexural strength reported in this study is similar to that of human trabecular bone (10-20 MPa) [26, 27]. The scaffolds with 0.4 vol. % of Ti fibers were found to have the highest fracture toughness ($\sim 0.8 \text{ MPa} \cdot \text{m}^{1/2}$) and scaffolds without fibers had a toughness of $\sim 0.5 \text{ MPa} \cdot \text{m}^{1/2}$. This trend can be attributed to the presence of high amount of Ti fiber content in the scaffolds with 0.4 vol. % fibers. The toughness of the scaffolds with 0.4 vol. % fibers is comparable to that of human trabecular bone (0.1-0.8 $\text{MPa} \cdot \text{m}^{1/2}$) [26, 27]. Both flexural strength and fracture toughness improved with the addition of Ti fibers.

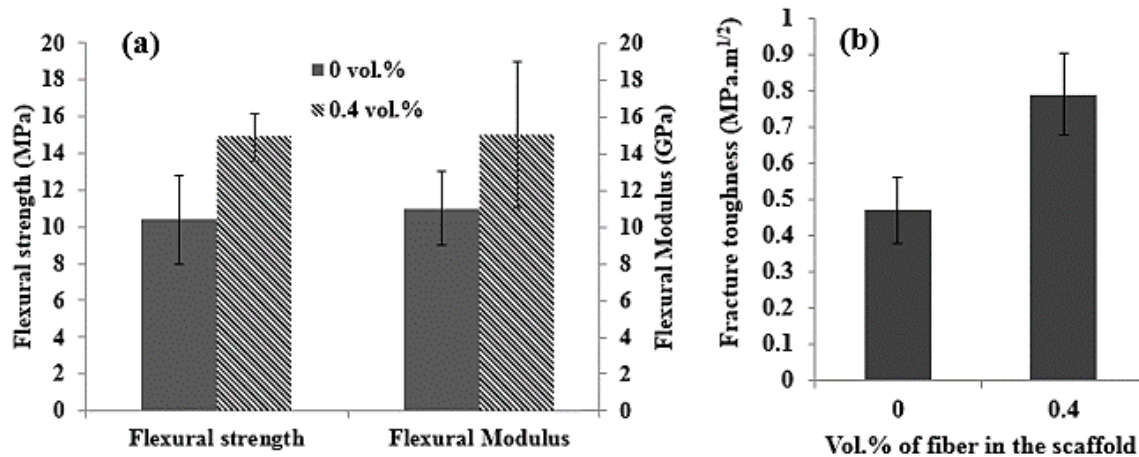


Figure 4: (a) Flexural modulus and flexural modulus (b) fracture toughness of scaffold without (0 vol. %) and with Ti fibers (0.4 vol. %)

Studies have shown that the mechanical properties of borosilicate glass matrix improved (five-fold improvement in fracture toughness) due to addition of Hastelloy X fibers (15 vol. %) in them [14]. XPS analysis performed on the fibers showed a presence of TiO_2 on the surface of the Ti fibers. The presence of a layer of TiO_2 could aid in bonding of the Ti fiber with the 13-93 bioglass matrix which predominantly consists of several oxides including SiO_2 . In addition, the rough and uneven surface of Ti fiber assists the bioglass matrix to better bond with the Ti fibers. An increased adhesion between the glass matrix and the Ti fibers will increase the strength of scaffolds [29]. Below a fine layer of TiO_2 on surface of the fibers, pure elemental Ti is present at the core. The Ti fibers have an average tensile strength in the range from 246 to 370 MPa which would help reinforce the brittle glass matrix by transferring the bending stresses from the matrix to the fibers [14, 28].

In this study, Ti fibers were added during the production of paste and not during the fabrication process. This type of pre-impregnation creates a homogenous matrix, which in turn increases the strength considerably as compared to when the fibers are added manually. Figure 5 shows the SEM images of the cross section of sintered pellets which shows the Ti fiber bonded to the glass matrix. The thermal expansion coefficient of Ti fibers and 13-93 bioglass are 8.6×10^{-6} m/m °C and 10.6×10^{-6} m/m °C respectively. After sintering, the glass matrix will be in contraction and the Ti fibers will be in tension, preserving the bond between the matrix and fiber. No fiber pullout was observed after the sintering process. The fibers in scaffold are expected to prevent crack propagation and thereby toughens the 13-93 bioglass matrix. For the scaffolds without any fibers, the cracks could easily propagate through the brittle matrix leading to fracture.

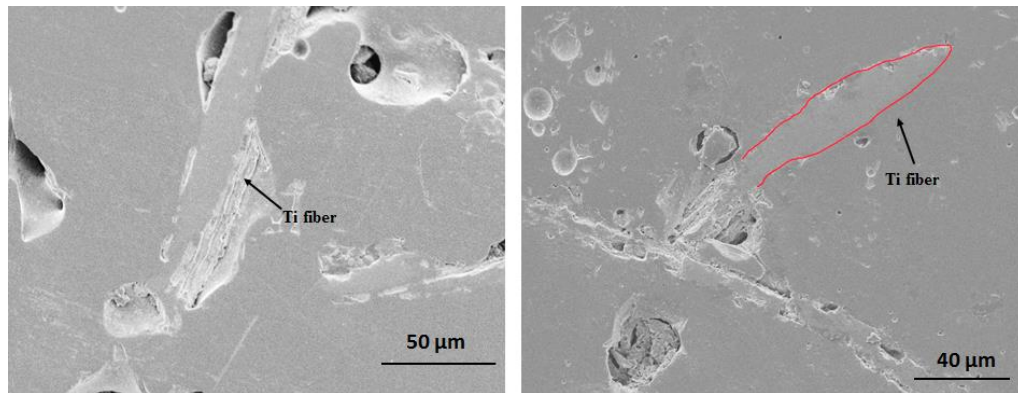


Figure 5. 13-93 bioglass-Ti fiber pellets showing good bonding between Ti fibers and glass matrix.

3.3. *In-vitro* evaluation of the scaffolds

Mechanical degradation of scaffolds without and with Ti fibers, as a function of immersion time in SBF is shown in Figure 6.a and 6.b respectively. The compressive strength of scaffolds without fibers, before immersion, was measured 103 ± 33 MPa. This strength was reduced to 67 MPa (~ 30 % reduction) following the immersion of scaffolds in SBF for four weeks. The strength of scaffolds with fibers before immersion was 128 ± 30 MPa. This strength was reduced by ~39% after 4 weeks to 88 MPa. The compressive strength reduced considerably in the first two weeks (~24 %). It was also observed that the reduction in strength is low from two to four weeks in comparison to the first couple of weeks (~10%). Such a reduction in the compressive strength is in accordance with similar results reported by researchers [5, 7, 8]. The compressive strengths of scaffolds with Ti fibers obtained even after four weeks of immersion in SBF was similar to that of human cortical bone proving the potential of the 13-93 bioglass + Ti composite system for load-bearing bone repair [26, 27].

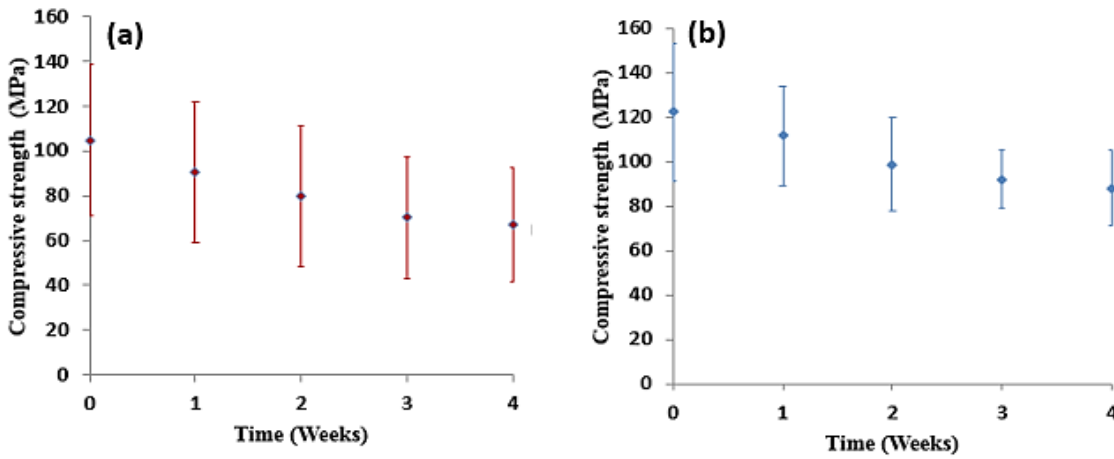


Figure 6. Variation in the compressive strength of the scaffolds after immersion in SBF for 4 weeks; (a) for scaffolds without fiber (b) scaffolds with fiber

The SEM images of scaffold surfaces, with and without fibers immersed in SBF for two weeks, are shown in Figure 7. Figure 7.a shows the SEM image of the surface of the dried scaffold without fibers, after it has been removed from the SBF and dried overnight. Surface of a scaffold with fibers immersed in SBF is pictured in Figure 7.b. No noticeable changes could be observed between the both sets of scaffolds. The surface cracks are typically formed because of the dried silica rich layer beneath the crystalline HA-like layer formed on the surface. Needle-like structures similar to that of HA were observed at a higher magnification (Figure 7.b) [3, 8, 12]. The XRD patterns of scaffolds (both with and without fibers) immersed in SBF had peaks that matched to the reference synthetic HA [24].

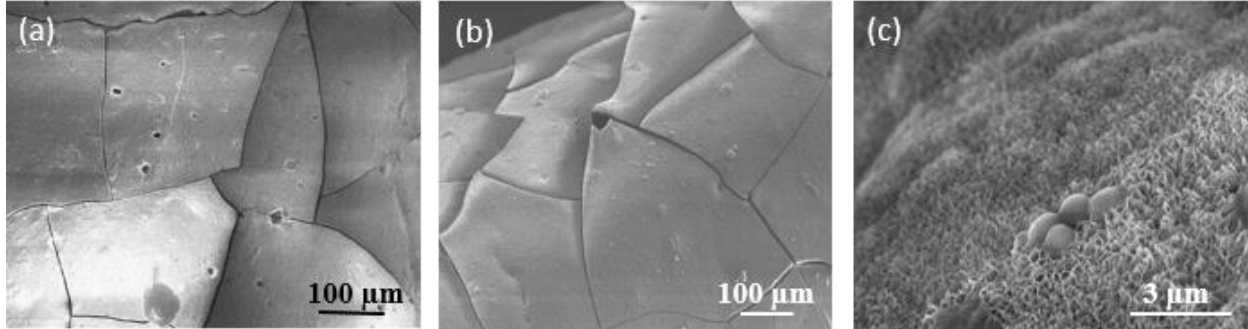


Figure 7. SEM images of surface of a typical scaffold (a) without fiber (b) with fiber after immersion in SBF for 2 weeks and drying; (c) needle like HA crystals formed on the surface (at higher magnification).

The formation of HA based on the SEM images and XRD patterns confirms the bioactivity of the scaffolds. When the 13-93 bioglass scaffolds are kept in SBF, Na^+ , K^+ and $(\text{SiO}_4)^4-$ ions are released into the solution. HA is formed due to the reaction of CaO present in the bioglass with phosphate ions in the SBF solution. The conversion of bioglass scaffold into HA also results in the reduction of its mechanical properties. Though the rate of degradation of silicate based 13-93 bioglass is slower because of its chemical durability. This can be observed in the reduction in compressive strength of the scaffolds after four weeks of immersion in SBF; See

Figure 5. Such a slow reduction in compressive strength of the scaffolds is a desirable property of bone implants. The scaffolds with fibers had an average compressive strength of ~88 MPa after immersion in SBF solution for four weeks. This finding leads to a possibility that these scaffolds could be used for load bearing applications in the body, as it is comparable to the that of human cortical bone (100 – 150 MPa) [26, 27].

4. Conclusion

This study investigated the feasibility of fabricating titanium fiber reinforced 13-93 bioglass scaffolds using freeform extrusion fabrication technique. Scaffolds reinforced with fibers had a fracture toughness of ~ 0.8 MPa•m^{1/2} and flexural strength of ~ 15 MPa. The fracture toughness of scaffolds with fibers increased by 70% compared to that without fibers and the flexural strength increased by 40%. The *in vitro* assessment of scaffolds revealed that the addition of biocompatible titanium fibers to the bioactive glass reinforced the scaffold mechanically without inhibiting its bioactive properties. The improved mechanical properties with compressive strengths of ~88 MPa even after four week degradation in simulated body fluid shows the potential of the 13-93 bioglass+Ti composite implants for load bearing bone repair applications.

5. Acknowledgment

This research was funded by the Interdisciplinary Intercampus Research Program of University of Missouri System and the Center for Biomedical Science and Engineering at the Missouri University of Science and Technology

References

- [1] Hench, L. L., Bioceramics: from concept to clinic. *J. American Ceramic Society*. 74(7), 1487-1510 (1991).
- [2] Fu, Q., Rahaman, M. N., Bal, B. S., Huang, W., & Day, D. E., Preparation and bioactive characteristics of a porous 13–93 glass, and fabrication into the articulating surface of a proximal tibia. *J. Biomed. Mat. Res. Part A*. 82(1), 222-229 (2007).
- [3] Liu, X., Rahaman, M. N., Fu, Q., & Tomsia, A. P., Porous and strong bioactive glass (13–93) scaffolds prepared by unidirectional freezing of camphene-based suspensions. *Acta Biomater.* 8(1), 415-423 (2012).
- [4] Kolan, K. C., Leu, M. C., Hilmas, G. E., Brown, R. F., & Velez, M., Fabrication of 13-93 bioactive glass scaffolds for bone tissue engineering using indirect selective laser sintering. *Biofabrication*. 3(2), 025004 (2011).
- [5] Doiphode, N. D., Huang, T., Leu, M. C., Rahaman, M. N., & Day, D. E., Freeze extrusion fabrication of 13–93 bioactive glass scaffolds for bone repair. *J. Mater Sci: Materials in Medicine*. 22(3), 515-523 (2011).
- [6] Fu, Q., Rahaman, M. N., Bal, B. S., & Brown, R. F., Preparation and in vitro evaluation of bioactive glass (13–93) scaffolds with oriented microstructures for repair and regeneration of load-bearing bones. *J. Biomed Mat Res Part A*. 93(4), 1380-1390 (2010).

- [7] Fu, Q., Rahaman, M. N., Bal, B. S., Brown, R. F., & Day, D. E., Mechanical and in vitro performance of 13–93 bioactive glass scaffolds prepared by a polymer foam replication technique. *Acta Biomater.* 4(6), 1854-1864 (2008).
- [8] Liu, X., Rahaman, M. N., Hilmas, G. E., & Bal, B. S., Mechanical properties of bioactive glass (13-93) scaffolds fabricated by robotic deposition for structural bone repair. *Acta Biomater.* 9(6), 7025-7034 (2013).
- [9] Liu, X., Rahaman, M. N., Liu, Y., Bal, B. S., & Bonewald, L. F., Enhanced bone regeneration in rat calvarial defects implanted with surface-modified and BMP-loaded bioactive glass (13-93) scaffolds. *Acta Biomater.* 9(7), 7506-7517 (2013).
- [10] Lin, Y., Xiao, W., Liu, X., Bal, B. S., Bonewald, L. F., & Rahaman, M. N., Long-term bone regeneration, mineralization and angiogenesis in rat calvarial defects implanted with strong porous bioactive glass (13–93) scaffolds. *J. Non-Crystalline Solids* (2015).
- [11] Velez, M., Jung, S., Kolan, K. C. R., Leu, M. C., Day, D. E., & Chu, T. M., In vivo evaluation of 13-93 bioactive glass scaffolds made by selective laser sintering (SLS). *Biomater Sci: Processing, Properties and Applications II: Ceramic Transactions, Volume 237.* 91-99 (2012).
- [12] Kolan, K. C., Leu, M. C., Hilmas, G. E., & Velez, M. Effect of material, process parameters, and simulated body fluids on mechanical properties of 13-93 bioactive glass porous constructs made by selective laser sintering. *Journal of the mechanical behavior of biomedical materials.* 13, 14-24 (2012).
- [13] Lin, Y., Xiao, W., Liu, X., Bal, B. S., Bonewald, L. F., & Rahaman, M. N., Long-term bone regeneration, mineralization and angiogenesis in rat calvarial defects implanted with strong porous bioactive glass (13–93) scaffolds. *Journal of Non-Crystalline Solids* (2015)
- [14] Boccaccini, A. R., Ondracek, G., & Syhre, C., Borosilicate glass matrix composites reinforced with short metal fibres. *Glastechnische Berichte.* 67(1), 16-20 (1994).
- [15] Trocynski, T. B., & Nicholson, P. S., Fracture Mechanics of Titanium/Bioactive Glass-Ceramic Particulate Composites. *Journal of the American Ceramic Society.* 74(8), 1803-1806 (1991).
- [16] Blaker, J. J., Nazhat, S. N., & Boccaccini, A. R., Development and characterisation of silver-doped bioactive glass-coated sutures for tissue engineering and wound healing applications. *Biomaterials.* 25(7), 1319-1329 (2004).
- [17] Gmeiner, R., Mitteramskogler, G., Stampfl, J., & Boccaccini, A. R., Stereolithographic Ceramic Manufacturing of High Strength Bioactive Glass. *International Journal of Applied Ceramic Technology.* 12(1), 38-45 (2015).
- [18] Elomaa, L., Kokkari, A., Närhi, T., & Seppälä, J. V., Porous 3D modeled scaffolds of bioactive glass and photocrosslinkable poly (ϵ -caprolactone) by stereolithography. *Composites Science and Technology.* 74, 99-106 (2013).
- [19] Cesarano, J., Dellinger, J. G., Saavedra, M. P., Gill, D. D., Jamison, R. D., Grosser, B. A., Sinn-Hanlon, J.M., Goldwasser, M.S., Customization of Load-Bearing Hydroxyapatite Lattice Scaffolds. *International Journal of Applied Ceramic Technology* 2.3: 212-220(2005).
- [20] Simpson, R. L., Wiria, F. E., Amis, A. A., Chua, C. K., Leong, K. F., Hansen, U. N., ... & Lee, M. W., Development of a 95/5 poly (L-lactide-co-glycolide)/hydroxylapatite and β -tricalcium phosphate scaffold as bone replacement material via selective laser sintering. *J. Biomed. Mat. Res. Part B: Applied Biomaterials.* 84(1), 17-25 (2008).

- [21] Kolan, K. C., Thomas, A., Leu, M. C., & Hilmas, G., In vitro assessment of laser sintered bioactive glass scaffolds with different pore geometries. *Rapid Prototyping Journal*. 21(2), 152-158 (2015).
- [22] Kolan, K. C., Leu, M. C., & Hilmas, G., Comte, T., Effect of architecture and porosity on mechanical properties of borate glass scaffolds made by selective laser sintering. *Proc. of the 22st Annual Int. Solid Freeform Fabrication Symp. Austin, TX*, 816-826 (2013).
- [23] Chen, Q. Z., Thompson, I. D., & Boccaccini, A. R., 45S5 Bioglass®-derived glass-ceramic scaffolds for bone tissue engineering. *Biomaterials*. 27(11), 2414-2425 (2006).
- [24] Kokubo, T., & Takadama, H., How useful is SBF in predicting in vivo bone bioactivity?. *Biomaterials*. 27(15), 2907-2915 (2006).
- [25] Kolan, K. C., Leu, M. C., & Hilmas, G., Velez, M., Effect of Particle Size, Binder Content and Heat Treatment on Mechanical Properties of 13–93 Bioactive Glass Scaffolds. *Proc. of the 22st Annual Int. Solid Freeform Fabrication Symp. Austin, TX*, 816-826 (2011).
- [26] M. Keaveny, W.C. Hayes, in: B.K. Hall (Ed.), Bone. A Treatise, CRC Press, Boca Raton, FL. pp. 285 (1993).
- [27] Fung, Y. C., *Biomechanics: mechanical properties of living tissues*. Springer Science & Business Media (2013).
- [28] Donachie, M. J., *Titanium: a technical guide*. ASM international (2000).
- [29] Yeomans, J. A., Ductile particle ceramic matrix composites—Scientific curiosities or engineering materials?. *Journal of the European Ceramic Society*. 28(7), 1543-1550 (2008).